Published in: 20th International Congress on Instrumentation in Aerospace Simulation Facilities ICIASF 2003 Record, Göttingen, Germany, August 25.–29. 2003, pp. 77 – 88

Transition Detection by Temperature Sensitive Paint at Cryogenic Temperatures in the European Transonic Wind Tunnel (ETW)

U. Fey, R. H. Engler,
Deutsches Zentrum für Luft- und Raumfahrt e.V. (DLR)
Bunsenstrasse 10, 37073 Göttingen, Germany
Y. Egami, Y. Iijima, K. Asai,
National Aerospace Laboratory of Japan (NAL)
7-44-1 Jindaiji-Higashi, Chofu Tokyo 182-8522, Japan
U. Jansen, J. Quest
European Transonic Wind Tunnel (ETW)
Ernst-Mach-Strasse, 51147 Köln-Porz

ABSTRACT

The identification of laminar-turbulent boundary layer transition on wind tunnel models provides essential data for modern wing design. However, simulating true flight Reynolds numbers with scaled models requires the use of cryogenic wind tunnels. Transition detection in 'warm' wind tunnels can be realized using commercially available IR cameras. In parallel, the temperature sensitive paint (TSP) technique is well established as an additional tool. In cryogenic testing, IR imaging becomes more difficult because of the reduction in radiated energy and the shift to longer wavelengths. Therefore, the TSP technique has become a promising alternative here. However, applying temperature sensitive paint in a large-scale cryogenic wind tunnel like the European Transonic Wind tunnel (ETW) needs specific modification of existing TSP formulations. Cooperative tests in the ETW therefore were performed by DLR and NAL (Japan). In these measurements, NAL's paint and DLR's mobile PSP/TSP system for data acquisition and evaluation[1,2,3] were used. Some efforts were made to adapt the system to specific conditions given at the ETW wind tunnel. So for the first time it was successfully realized to perform a TSP luminescent paint test at cryogenic temperatures in a commercial wind tunnel.

Nomenclature

Re	= Reynolds number
Ma	= Mach number
p_t, T	= stagnation pressure/temperature in tunnel
ΔT	= total amount of temperature change
δT	= temperature difference on wing
α	= angle of attack
C_L	= lift coefficient
x^*, y^*, z^*	= wing coordinates
s	= half wing span of model
η	= normalized spanwise coordinate (y^*/s)
x/c	= normalized chordwise coordinate

THE CRYOGENIC WIND TUNNEL

The European Transonic Wind tunnel (ETW) sited in Cologne, Germany, is an industrial cryogenic pressurized facility. It provides the capability for achieving full scale flight Reynolds numbers of transport aircraft by testing at pressures between 125 and 450 kPa and at temperatures between 110 and 310 K, using nitrogen as the test gas. The tunnel started operation in 1994, and, after a phase of commissioning and evaluation, it is available for productive testing since 1996[4].

Aerodynamic Circuit

The ETW has a closed aerodynamic circuit contained inside an internally insulated pressure shell. The two stage, fixed blade compressor are driven by a 50 MW synchronous motor. To achieve the desired low temperatures of the test gas, *liquid* nitrogen is injected continuously into the tunnel upstream of the compressor. The corresponding *gaseous* nitrogen exhaust upstream of the stilling chamber is controlled by valves for the accurate maintenance of tunnel pressure. From the settling chamber equipped with a honeycomb and anti-turbulence screens, the flow enters the test section via a flexible nozzle of contraction ratio 1:12 (Fig.1).

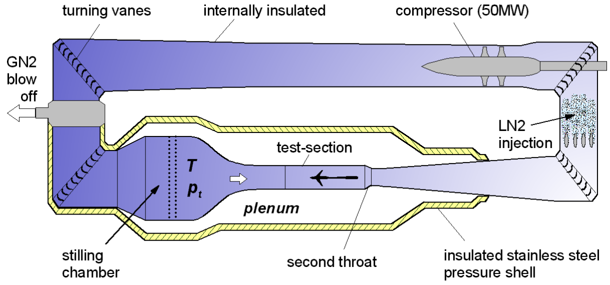

Figure 1: Aerodynamic circuit of the ETW wind tunnel. LN2: liquid nitrogen, GN2: gaseous nitrogen.

The test section has slots in the top and bottom wall for full span model tests and slotted side walls for half model tests. Mach number control can be achieved by three different operating modes: a) rpm settings of the compressor, b) formation of a sonic throat downstream of the test-section (only for $0.65 \leq Ma \leq 1$) and c) adaptation of circuit losses by trim flap setting in the second throat area.

Model Handling

As a consequence of using low temperature gaseous nitrogen as the test gas, two serious operational difficulties arise: The first problem is the accessibility of the model inside the test section for quick changes between runs, the second one is the risk of frost generation on the model surface when the model temperature is below the dew point of the test gas. Preparation of the model is done under ambient air conditions using a model cart positioned in a 'Cart Rigging Bay' (CRB). The whole set-up including model, model support, upper test section wall (top wall) and instrumentation cabin is then moved via a lock into an area of very dry air. Here it can be checked out under cold conditions before it is transported to the test section (Fig.2).

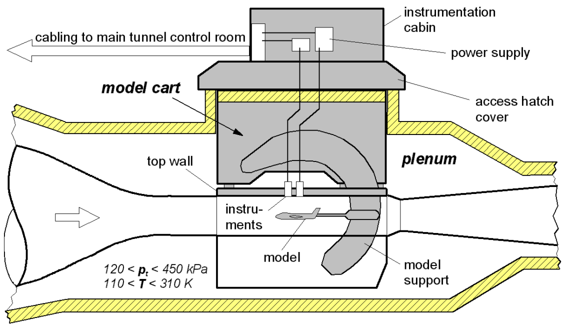

Figure 2: Model cart in the test section position of the wind tunnel. The complete part under the access hatch cover is cooled down during test runs. The whole assembly (gray area) can be transported to other locations (VTCR, CRB)

For a quick change, the model cart needs to be moved from the test section position into a 'Variable Temperature Check out Room' (VTCR). Here the model can be warmed up within an hour (starting from T=110K) and is subsequently accessible for modifications. In detail, this is realized by closing thermally insulated 'ceiling doors' in the VTCR directly beneath the top wall. Thus, the model can be warmed up using hot air blowers but leaving the complete upper part of the model cart at low temperatures. Consequently, this means that all instruments which are mounted in the top wall can not be accessed after a cool down of the tunnel. In case of failures, there is no chance to check the equipment on site and testing will consequently delayed to the required warm up of the complete model cart.

TSP METHOD

Temperature sensitive paint (TSP)[5,6] is a thin paint layer containing luminescent material (luminophore) within the binder. When the luminophore is activated by an excitation light source it emits some light at longer wavelengths (fluorescence). In the case of TSP, radiation intensity is temperature dependent and the underlying phenomenon is known as thermal quenching. Generally, luminescent intensity of TSP decreases with an increase in temperature. Some Ruthenium complexes are suitable as a luminophore for cryogenic testing because they exhibit high temperature sensitivity in the range of 90 to 200K.

Transition detection by TSP is based on recording the temperature difference δT between the laminar and turbulent regime of the boundary layer on a wing's surface which undergoes transition. The adiabatic wall temperature difference across transition line is estimated to be less than 0.5K at transonic speeds[7]. It is difficult in *steady* conditions to detect this small variation in boundary layer temperature due to heat conduction through the models surface[8].

Nevertheless, the thermal signatures across transition lines can be amplified by artificially increasing the temperature difference between the laminar and turbulent part of the boundary layer[9]. This is done by introducing a quick temperature change into the tunnel flow (temperature step). The convective heat transfer coefficient κ in turbulent flow is much higher than that in laminar flow. Therefore, within the turbulent boundary layer a temperature *change* in the outer flow is transferred faster onto the paint, giving an increased temperature difference δT during the step change. The transition line can be seen as the borderline between light and dark areas in the TSP image (Fig.3).

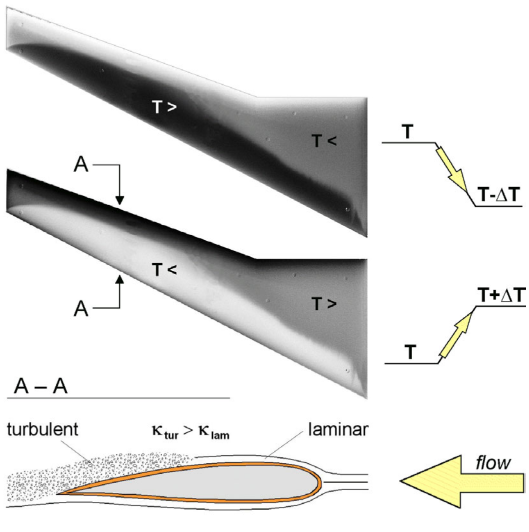

Figure 3: Principle of TSP measurement. A change in flow temperature amplifies the temperature difference on the wing.

Adaptation of TSP to Large Cryogenic Wind Tunnels
NAL (Japan) has developed a new temperature sensitive paint formulation[10] optimized for tests in large-scale cryogenic wind tunnels such as the European Transonic Wind tunnel (ETW) and the National Transonic Facility (NTF). In comparison to 'warm' and/or small wind tunnels, TSP for large cryogenic wind tunnels has to exhibit the following properties:

• Higher luminescent intensity (due to larger distances),
• Stronger coating robustness (due to strain during cool down and warm up),
• Reduced surface roughness (due to the small boundary layer thickness at high Reynolds numbers).

The new cryogenic TSP based on a Ruthenium complex was developed to meet the above requirements and was made compatible with DLR's mobile PSP/TSP measurement system and optimized for the ETW tests. The wavelength ranges for excitation and emission of the luminophore were given as $425 < \lambda_{exc} < 525$nm and $580 < \lambda_{em} < 680$nm, respectively.

MODIFICATION OF PSP/TSP SYSTEM

For executing TSP measurement besides the paint, a suited light source and a CCD camera along with proper optical filters are needed. The following describes, how camera and lamp are implemented into the ETW wind Tunnel.

Because of the limited space for installing equipment above the upper wall of the test section (top wall), instruments have to be mounted in so called 'standard housings' whenever possible (Fig.4).

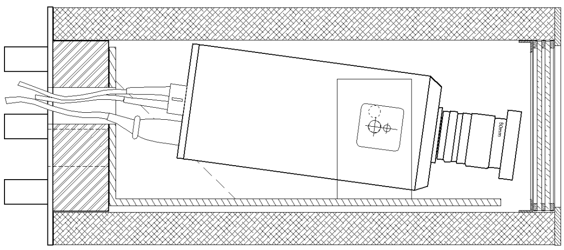

Figure 4: Sketch of TSP camera implemented in the ETW standard housing (thermo box).

A standard housing is a heated stainless steel box of outer dimensions 42cm × 20cm × 20cm. In between the outer shell and the inner surface there is 3cm of thermal insulation. The front end of the box is equipped with two quartz glass windows. The inner wall of the box is covered with heating foils which are part of a feedback control system which in addition consists of Pt100 temperature sensors and a thermostat. Thus, the temperature within the housing can be maintained within a given range (for example $20^{o} < T_{housing} < 25^{o}C$) during tunnel operation at low temperatures. It should be pointed out, that a standard housing is not pressure proof. Therefore cameras and lamps were designed also for high pressures up to 450 kPa.
All instrumentation cabling was routed to the back of the housing and is exposed to cryogenic atmosphere in the model cart (see Fig.2). On the top of the model cart, it has to pass a thermal and a pressure lock and thereafter can be connected to other devices in the instrumentation cabin. These units can be read out and controlled from the main tunnel control room (MTCR) which is located in a large distance apart from the wind tunnel itself.

Development of a New Excitation Light Source
In co-operation with an industrial lamp designer, a new excitation lamp was developed with respect to the following attributes:

• Power supply and flash lamp unit should be decoupled to avoid the need for a 'non-standard' housing,
• Flash energy should be as high as possible,
• In a distance of 1m, an area of $\sim 1m^2$ should be illuminated with a homogeneous intensity distribution,
• Optical Filters (used for selecting of desired wavelength ranges) should easily be changeable.

The above specifications were realized by building a 'lamp-head' integrated into a standard housing and a detached power supply unit, which can be mounted into a common 19´´ rack in the instrumentation cabin. The power supply device (and thus, the flash lamp) can be triggered using a TTL signal generated by a PC in the main tunnel control room. The lamp-head consists of two linear Xenon flashbulbs, mounted within a parabolic reflector (Fig.5).

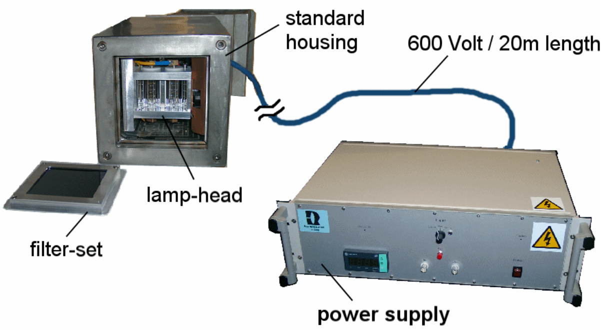

Figure 5: Excitation light source consisting of a lamp-head with Xenon flashbulbs and a decoupled power supply.

The location of the bulbs with respect to the reflectors can be adjusted within a certain range. In addition, capacitors for the flash lamps are mounted nearby in the lamp-head as well as all corresponding electronics. The capacitors are charged using a 600 Volt feed-line connected to the power supply in the instrumentation cabin. With this lamp device, a maximum flash frequency of 40Hz was realized.
The desired wavelength range out of the Xenon spectrum is selected by mounting a suitable filter combination in front of the flash bulbs. Special care was taken to make the lamp-head leak proof to avoid other wavelengths passing the housing which would have disturbed the measurement. All filters were special designs of dimensions 10cm × 10cm, considering angular dependence of filter characteristics. For later PSP measurement in the ETW, the filter-set can be easily replaced. In case of TSP measurements, a filter-set of three different glasses was used, selecting the range 425 < λ_{exct} < 525nm for excitation of the luminophore within the TSP layer.

Implementation of the CCD Camera
The CCD camera of DLR's mobile PSP/TSP system[2,3] just fits inside a standard housing box. Great care was taken to fix the camera in position, since it is influenced by vibrations during the transportation of the model cart or during operation of the wind tunnel (Fig.6). In addition, all movable parts on the objective (aperture, focussing ring and filter frame) were fixed as well. If anything would be dissembled during test runs, there would be no chance to readjust it.

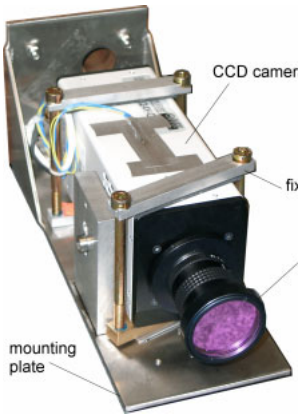

Figure 6: Camera mounted on the housing's mounting plate with a filter in front of the objective lens.

A cooled black-and-white OMT-1024Y CCD camera was used with spatial resolution of 1280×1024 pixels and 12bit dynamic range. The CCD chip is cooled down to ~ –15°C during operation to guarantee low background noise.

Image data is transferred to a data acquisition PC in the main tunnel control room using fiber optics. This is a necessary feature since the cabling has to bridge a large distance from the camera to the PC. The power supply for the camera is mounted into the instrumentation cabin and can be remotely controlled by the tunnel control system. An interference filter is mounted in front of the lenses, selecting the wavelength range 580 < λ_{em} < 680nm which corresponds to the temperature sensitive emission band of the TSP luminophore.

ETW Reference Model
The ETW reference model is a scaled version of a test configuration known as DLR F4 fuselage-wing assembly (scaling factor 1.225). It was selected as a test model in the present experiments, since there exists a huge database containing IR imaging of transition line, pressure measurements in different wind tunnels as well as results from numerical simulations. The model was made of stainless steal and has a polished surface. Prior to applying the TSP layer, the center part of the body and both wings were painted with ETW's white layer. This deposit establishes thermal insulation and serves as a screening layer. After curing, the white layer was polished and the model stored until TSP application. Before spraying the TSP layer some marker positions were created by painting dots on the white layer. In the acquired raw images, these positions can be seen as black spots. Markers are needed to carry out image alignment during 2D, and especially during 3D evaluation.

Setup for TSP Measurement
The camera and lamp are separated by 42cm when they are mounted in the 'structure' of the upper wall of the test section. Therefore, the lamp-head was mounted slightly inclined with respect to the perpendicular to improve illumination of the wing (Fig.7).

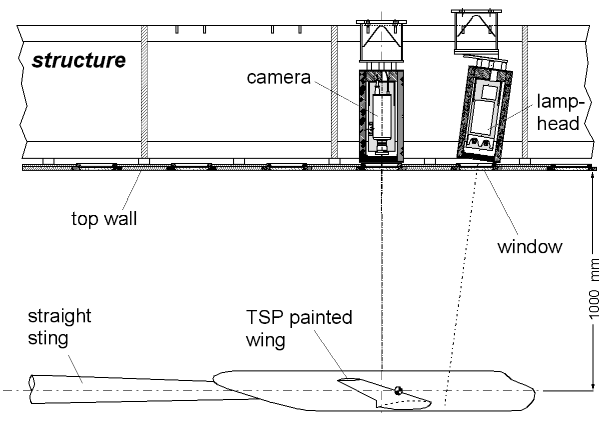

Figure 7: Setup for TSP tests with ETW reference model.

In front of each housing, two quartz glass plates terminate the box which are separated by 3mm (see Fig.4). Within the structure, the housings are mounted such that this window is directly above a corresponding window of the top wall. All glass plates were covered with an anti-reflection coating and the windows on the lamp side are made out of UV permeable quartz glass (compatible with future PSP tests). The camera shutter and the flash lamp can be triggered simultaneously by the PC in the main tunnel control room.

Mock-up

It is rather difficult to access the structure of the top wall in ETW, where all instrumentation for the TSP test had to be mounted. Further, it would be very time consuming to do adjustment of cameras and lamps when they are already installed in the top wall within their housings. Therefore it was decided to build a mock-up of the top wall, reconstructing part of the structure at a scale 1:1 at DLR Göttingen (Fig.8).

In addition, a 'dummy' model of the ETW reference model was built to have the possibility to test flash lamp and image acquisition with the same alignments as used for the ETW tests. All adjustment of camera and lamp was done using the mock-up at DLR where the 'cloned' structure is easily accessible. Finally, the fixed instruments within their housings were transported to ETW where they simply had to be mounted into the top wall structure without doing any additional adjustment. This strategy worked very well for these TSP tests.

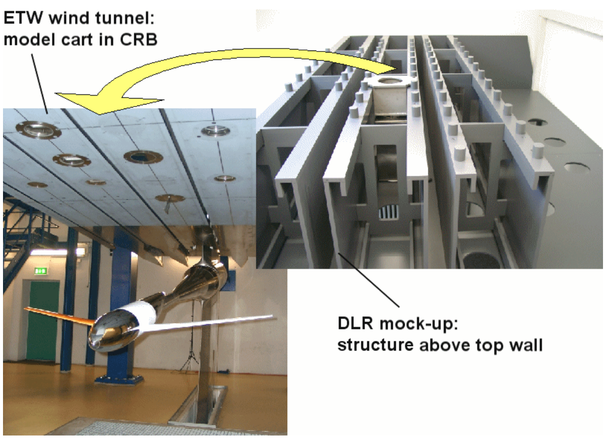

Figure 8: Model Cart at ETW- and Mock-up at DLR side. All adjustment of camera and lamp was done using the mock-up.

TEST EXECUTION

This first test series was carried out under the co-operation of DLR, ETW and NAL (Japan). The TSP paint was provided and prepared by NAL[10]. A white primary paint layer was already applied to the model as described. The upper side of the starboard wing including the leading edge was painted with the new TSP by an industrial sprayer. Simultaneously, a stainless steel sample plate was sprayed which was later used for calibration tests in a cryogenic calibration chamber at DLR. The result of this calibration shows a good sensitivity in the range 90 < T < 200K and nearly linear temperature dependence from 110 to 170K (Fig.9).

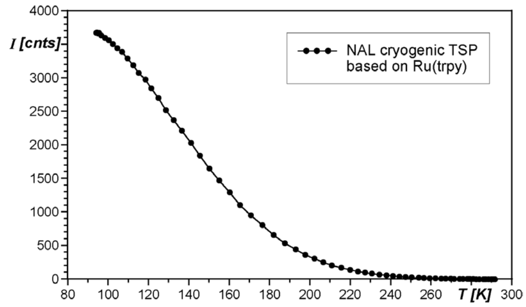

Figure 9: Calibration curve for TSP paint. Intensity values (I) within the CCD images of the sample were measured as a function of temperature. Excitation was done by the new flash lamp and filter.

After being cured for 2 days, the painted wing surface was carefully polished with aluminum oxide lapping sheets. Consequently, the surface of the TSP layer was finished to less than 0.05µm (R_a-value) which is three times 'smoother' then the value specified by ETW (0.15µm). After polishing, the model was mounted on the straight sting of the model cart. In parallel, the camera and excitation light source were mounted into the top wall (within their housing, see Fig.7) and checked for functionality. After rigging, the model cart (including model, top wall and instrumentation) was transported to the tunnel, passing the lock before entering the dry air region.

Two months later, a second model test using the same TSP coating was accomplished in the ETW. The second test had two principle aims: Firstly to check the ageing of the paint after two months of storage. Secondly to investigate the influence of a leading edge region without paint. The paint at the nose of the wing can sometimes be hit by dust particles during testing, which can create impact holes. Impacts mark small disturbances which can trigger transition of the flow at the leading edge region. They can be seen in the resulting images as wedge shaped patterns originating directly on the

leading edge. In the second test, therefore, the paint was removed from this part of the wing, having in mind that a blank stainless leading edge is less susceptible to impact damage, thus, giving less turbulent wedges.
Just before the second test campaign the existing impact holes which occurred after the first test were filled up and the nose region polished again. After one day of testing, the model cart was moved to the VTCR and the paint was removed from the nose of the wing. Using this configuration, some data points were repeated.

Table1 in summary shows the test cases covered for the two TSP campaigns. The corresponding Mach number is 0.785 which is equal to the design Mach number for the model. At the end of the first test, the tunnel was pumped up to 450 kPa at T=120K to check the camera and lamp devices (within their heated housing) under these extreme conditions. DLR's adapted camera and the newly designed flash lamp passed this test without causing problems.

1st test				2nd test			
C_L	Re' [10^6]	T' [K]	p_t [kPa]	C_L	Re' [10^6]	T' [K]	p_t [kPa]
0.5	6	170	121	0.5	6	170	121
0.5	12	120	144	0.5	10	170	210
0.5	12	170	239	0.4	6	170	121
0.5	17	120	204	0.0	6	170	121
0.5	17	140	241	0.5	6 pLE	170	121
0.3	6	170	121	0.5	10 pLE	170	210
0.3	6	170	121	0.5	14 pLE	170	280
0.0	28	142	400	0.4	6 pLE	170	121
				0.0	6 pLE	170	121

Table 1: Test conditions for TSP tests. Test cases with paint removed from the wing's nose are indicated by pLE ('paintless' leading edge).

Creating Temperature Changes in ETW

During both tests, positive as well as negative temperature steps of $\Delta T = 4$, 8 and 12K were used for transition detection while the influence of ΔT on the resultant images was analyzed systematically during the first test. Realizing a positive step simply means to stop the nitrogen supply for a couple of seconds. The flow warms up caused by the heat input of the compressor. On the other hand, negative temperature steps were established by increasing the amount of injected liquid nitrogen (LN2).
When introducing a temperature step into the tunnel flow, the start-temperature and end-temperature were chosen such that the set point temperature T′ was in the middle of the covered range. For example, $\Delta T = +12K$ and T′= 170K means, that a step was realized starting from T=164K increasing temperature up to 176K. The temperature curve for $\Delta T = +12K$ in comparison to the –12K step (at a set point value of 170K) is shown in Figure10 for a Reynolds number Re′= 6 $\cdot 10^6$. Here, t* denotes a time scale with an arbitrarily chosen zero point. In addition to the flow temperature, the wing temperature during the step change is plotted which is given by a Pt100 sensor installed inside the TSP painted wing.

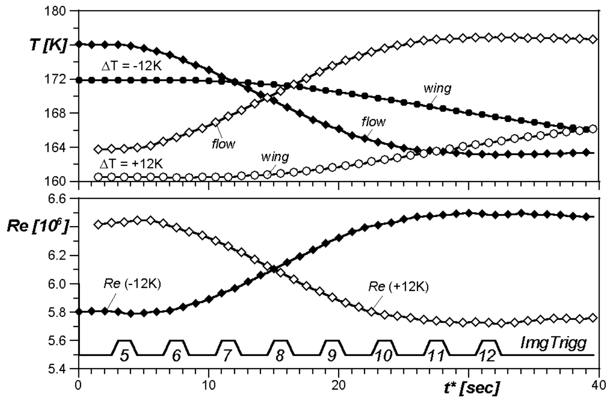

Figure 10: Comparison of positive (open symbols) and negative (black symbols) temperature steps. ΔT=12K, Re′= 6 $\cdot 10^6$. Reynolds numbers are based on the mean chordlength of the model c′ = 0.173m.

The lower graph in Figure 10 includes the trigger signal (ImgTrigg) which controls the camera and in parallel opens the gate for the excitation flash lamp. During the gate open, the lamp operates with a constant flash frequency of 16Hz. Besides aperture and focal length of the objective used with the camera, the image exposure time depends on the tunnel temperature and was within the range 0.5sec for T′=120K to 1.5sec for T′=170K. Delay time between single images was 4sec.

The procedure of TSP image acquisition was as follows: When the tunnel flow had reached stable conditions for the start-temperature, an image series was initiated whereby 12 consecutive images were taken. This is controlled by the PC using a trigger signal. The first four images were taken under a stable condition and represent a series of reference images.
After acquisition of image No.4, the tunnel control system starts a temperature step. Images from No.5 to No.12 are taken during the increase or decrease in flow temperature (see Fig.10). Mainly at the beginning of a temperature step, the Mach number and total pressure change slightly until the tunnel control system brings them back to a constant value. These deviations were smaller then 0.8% throughout the tests. During the second test, an additional effort has been undertaken to minimize these effects.

In Figure 11, the raw image No.10 out of the series for ΔT= +12K is shown. For this temperature step and Re′= 6 million, the signature of the transition line can already be seen in the raw image. This was not the case for the smaller temperature steps or for the higher Reynolds numbers. In these cases, it was necessary to take the *ratio* of the series images with respect to the reference image to highlight the transition pattern.

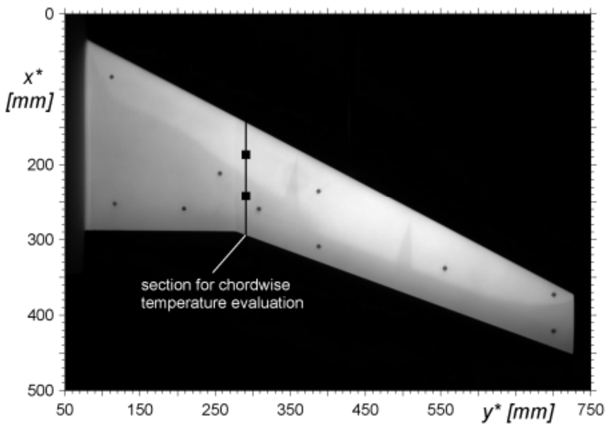

Figure 11: Raw image No.10 for $\Delta T= +12K$ ($Re = 5.83 \cdot 10^6$). The black spots on the wing indicate the marker positions.

A section was selected at a spanwise position of $\eta=0.40$ ($y^* \approx 290mm$ in Fig.11) to determine the chordwise temperature distribution for $Re' = 6$ million and $\Delta T = \pm 12$, 8, 4K. It is assumed, that the boundary layer temperature is near the total temperature when starting the step change (i.e. during acquisition of reference images). Using the calibration for the TSP paint (see Fig.9), it was possible to calculate the absolute temperature distribution from the intensity values given in the image. Figure 12 shows the results for the image series taken at $Re' = 6$ million and using $\Delta T= +12K$.

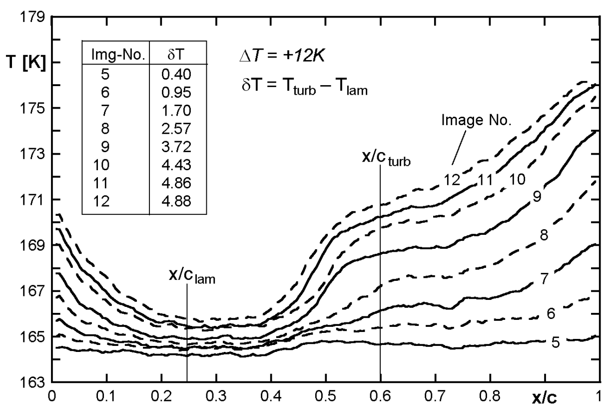

Figure 12: Chordwise temperature distributions at $\eta=0.40$ and for $Re' = 6 \cdot 10^6$ ($T'=170K$, $p_t = 121$ kPa, $\Delta T= +12K$).

The temperature differences $\delta T = T_{turb} - T_{lam}$ were calculated for images No.5 to 12 with T_{lam} taken at x/c = 0.25 and T_{turb} at x/c =0.6 (indicated by the black squares in Figure 11). A comparison of positive temperature steps $\Delta T= +12$, +8, +4K is given in figure 13. Here, the temperatures for laminar and turbulent parts of the boundary layer are evaluated using images No.10 out of the corresponding image series. Regarding the evaluation of the *negative* temperature steps, it is possible to state that, in all cases, δT is of the same order of magnitude, but with opposite sign in comparison to the data in Figures 12 and 13. This fact is not self-evident, since the realization of positive and negative steps can be different in other wind tunnels.

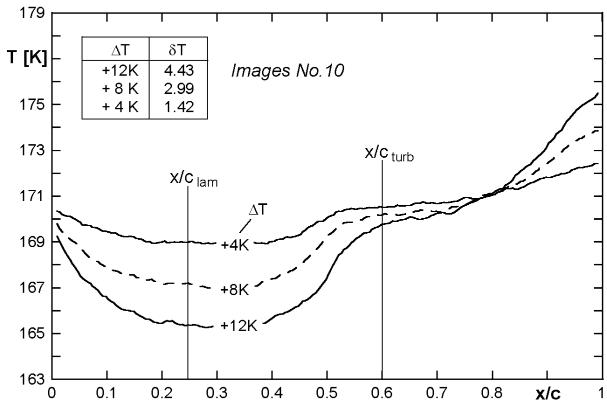

Figure 13: Temperature distributions for $\Delta T= +12$, +8, +4K and for $Re' = 6 \cdot 10^6$.

For example in the NAL 0.1-m transonic cryogenic wind tunnel[9] (0.1-m TCWT) the establishment of a suited positive temperature step was more difficult to realize since the fan power is relatively small compared to ETW. When the ETW wind tunnel operates at lower flow speeds (for example Ma = 0.2), the same fact holds true. A positive step at Ma=0.2 takes more than one minute until the end-temperature is reached whereas a negative step can be performed in nearly the same way as for Ma=0.785.

In summary, the characteristics of positive and negative steps depends on the individual wind tunnel facilities as well as on the Mach numbers.

RESULTS

In the following transition images which are a result of the TSP evaluation are shown. This means, that raw images from No.5 to 12 out of an image series were rationed to a corresponding reference image. The reference image was given by averaging the four images from No.1 to 4 in each series which are taken under stable condition. Both series images and the averaged reference image were previously adjusted by subtracting a dark image. This dark image was calculated as the average of a series of images taken before each test run without light. The reason for subtracting a dark image is to remove background noise. The resulting ratio images were subject to some image enhancement to highlight the transition pattern on the wing's surface. Furthermore, a suited color palette is added to the result images. The information concerning the absolute temperature distribution was not calculated for these results since the primary interest was the location of the transition line, which is not influenced by the evaluation.

It is important to emphasize in the following description that in the case of negative temperature steps an inverted color palette was used in comparison to the positive steps. The reason is that it is easier to compare images taken at +ΔT with images taken at -ΔT without the confusion caused by the reversed colors on the wing (see Fig.3).

Comparison of Results for Positive and Negative ΔT

A complete evaluated image series for Re´= 6 million using ΔT= +12K is shown in Figure 14. Increase in temperature is from top to bottom and from left to right. It can be seen, that within the first four result images (No.5 to 8) the signatures on the wing surface becomes more and more visible due to an increase in temperature difference δT. At the end of the temperature change, a more and more darker area near the trailing edge of the wing occurs (wing images No.9 to 12). This is caused by heat transfer from the flow to the wing. The TSP layer itself and the underlying white layer give thermal insulation to the wing. However, some heat is transferred from the boundary layer to the wing substrate.

Since the wing is very thin near the trailing edge, there is not much (metallic) thermal mass of lower temperature which cools the paint layer from underneath. Therefore, the stainless steel warms up at the trailing edge which also results in a temperature increase within the paint layer. The same holds true for the leading edge but the effect is much smaller because of its different curvature. Despite this fact, the pattern seen in the images in Figure 14 seem to remain stable during the establishment of the temperature change. The wedge shaped pattern represents premature transition, caused by inhomogeneity on the nose of the wing (dust particles, impact holes or roughness).

Figure 15 shows the result images for the series taken at the same Re´ (6 million) but for the negative step ΔT= -12K. A comparable Reynolds number range is covered by the negative temperature step but the resulting images look completely different (note, that the image series for +12K and –12K were acquired shortly one after the other in the same test run).

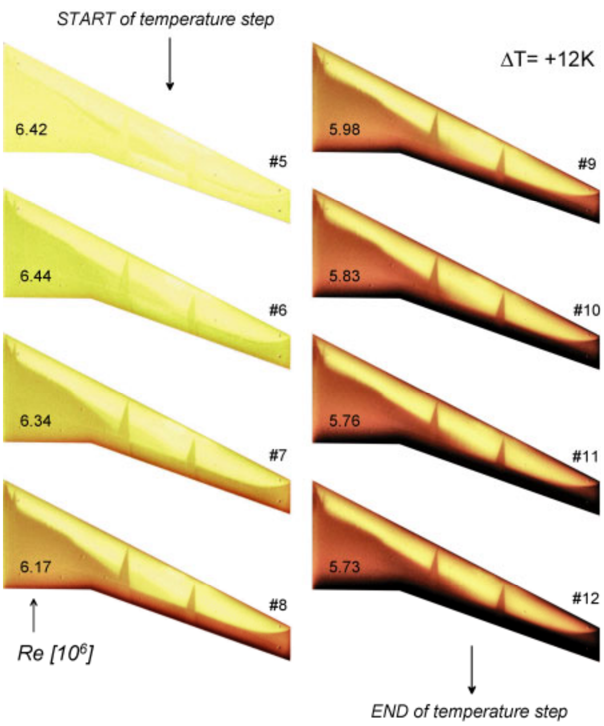

Figure 14: Result images for Re´= 6 $\cdot 10^6$ and positive temperature step ΔT= +12K. Ma=0.785, p_t= 121kPa, C_L = 0.5, α = -0.87°, T= 164 → 176K.

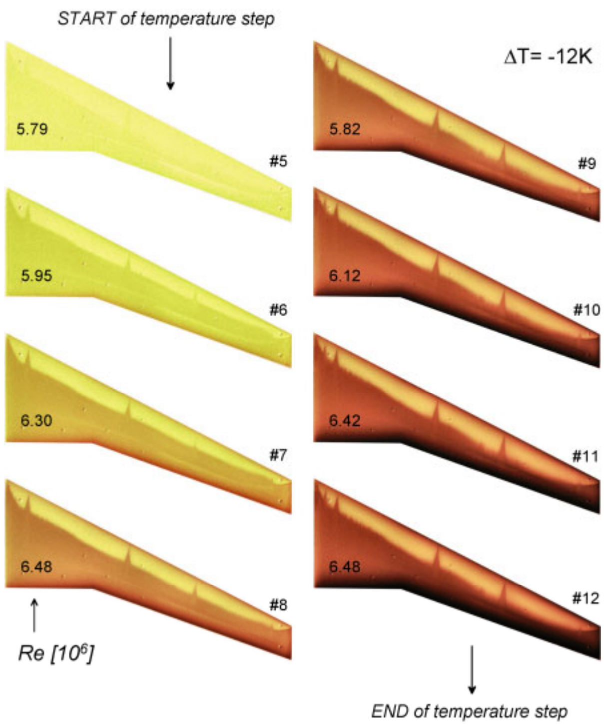

Figure 15: Same as in figure 14 but for negative step change ΔT= -12K (T= 176 → 164K). Color palette was inverted.

In comparison to the images taken with the positive step (Fig.14), the laminar-turbulent boundary layer transition is located more upstream in case of the negative step (Fig.15). The two turbulent wedges in the middle of the wing remained, one additional wedge occurred at the nose near the root of the wing. When inspecting the images carefully one can also find, that the transition line itself is more 'jagged' in the negative step images, especially in the region near the wing root.

In the images taken with ΔT= -12K one can see a line structure within the turbulent part of the boundary layer, appearing slightly brighter than the ambient area. The location of this line seems to be near by or at the same location where the boundary layer transition is given in the case of ΔT= +12K. To highlight this fact, two result images for nearly the same Reynolds number are selected (No.9 from Fig.14 and No.6 from Fig.15). They are shown in direct comparison in Figure 16. The lower wing image was subject to some further image enhancement to emphasize the described line patterns (arrows).
The arrangement in Figure 16 clearly shows that the line on the right in the lower image (right arrow) corresponds to the separation line in the upper wing image. Furthermore it is known from other experimental data and numerical results, that for the DLR F4 wing there is a weak shock on the upper surface at Ma = 0.785 and for C_L = 0.5. Following some contrast enhancement in other result images (for different Re´ and negative temperature steps), similar lines can be seen.

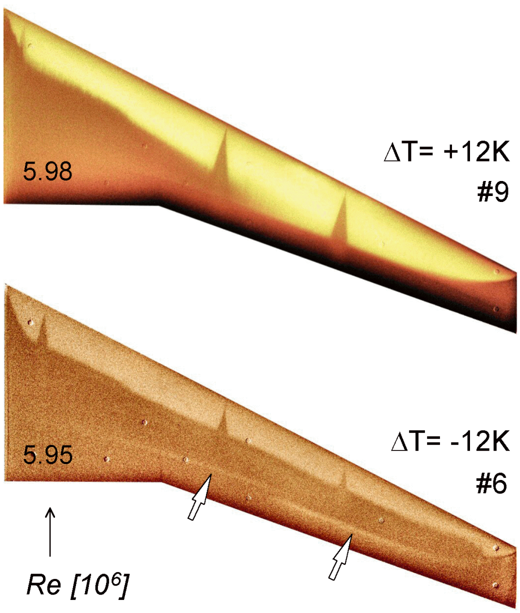

Figure 16: Direct comparison of ΔT = +12K to -12K. Arrows in the lower image denotes appearance of shock lines.

They always appear at the same location, independent of Reynolds number. Therefore, it may be possible to conclude that the shock line on the upper surface of the wing can be seen in the lower wing image in Figure 16.

In summary, for Re´= 6 million, the two different temperature steps of 12K show a shock induced separation of the boundary layer in the tip region for ΔT= +12K and an earlier transition in the case of ΔT= -12K located more upstream. The transition signatures near the wing's root look nearly the same in both cases.

There are three possible reasons to explain these facts:

1. Since the negative step in ETW is realized by an increase in LN2 injection, an increase in turbulence level of the flow may result, which may cause earlier transition in comparison to the positive step (which is realized by stopping LN2 injection).
2. In the case of the negative step, a heat transfer from the wing to the flow is given, since the wing becomes warmer with respect to the flow. This heat flux could force the boundary layer flow to become unstable more upstream.
3. In the case of the positive step the heat flux from the flow to the wing results in a stabilization of the boundary layer, which then separates induced by the shock.

Therefore, the question arises "Which temperature step has to be chosen to see the 'real' boundary layer transition on the wing, without being influenced by the direction of the temperature step?"

To answer this question, temperature steps of ±8K and ±4K are shown in direct comparison in Figures 17 and 18, respectively. It can clearly be seen, that with decreasing amount of ΔT, the difference between positive step images and negative step images vanishes. For example, for ΔT= ±8K, the lower wing image in Figure 17 still shows a shock line (arrow) but the boundary layer separation ahead of it. In the upper wing image of figure 17, a straight separation line can be seen but no shock. The difference between images taken at +8K and -8K is not as striking as in Figure 16, where signatures for ΔT= ±12K are shown.

Using ΔT= ±4K (Figure 18) it is hard to find any difference between positive and negative temperature step images. This also holds true when comparing both complete image series (not shown in this paper).
A temperature step of 4K gives minimum disturbance to the flow in the ΔT range investigated and hence, less influence on the boundary layer instability. However, the +ΔT images as well as the -ΔT images for 4K are very similar to the result images given by the +12K

temperature step (compare Fig.18 to Fig.14). This leads to the conclusion, that a *positive step* has the smallest influence on the transition process and that positive steps around 8 to 12K should be used for transition detection in ETW for Mach numbers around 0.785 (temperature steps of 4K give insufficient contrast for the higher Reynolds numbers). Therefore, the result images shown in the following are all taken from a series where a positive temperature step was used.

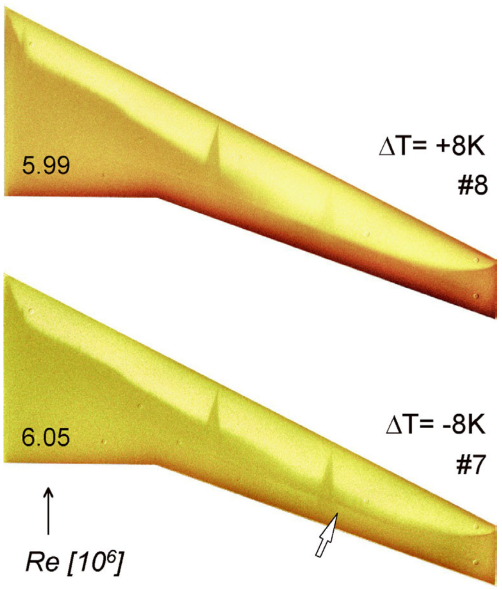

Figure 17: Comparison of +ΔT and -ΔT with ΔT= ±8K. Arrow in the lower image denotes location of shock.

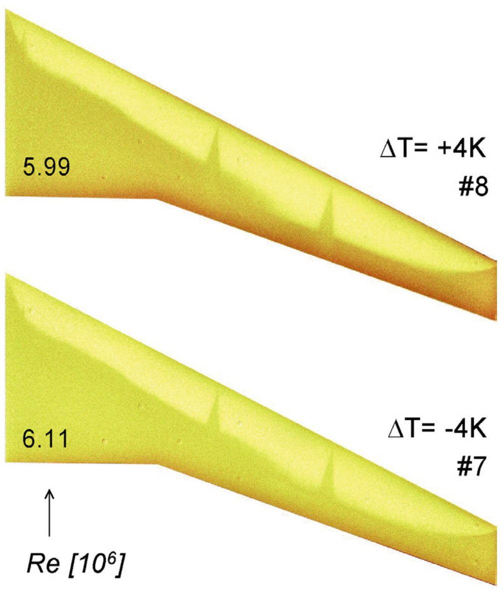

Figure 18: Comparison of +ΔT and -ΔT with ΔT= ±4K.

<u>Transition Pattern for Increasing Reynolds Number</u>

The development of the transition line on the upper surface of the wing with respect to Reynolds number is shown in <u>Figure19</u>. Compared to Re´= 6 million (upper wing image), the transition 'line' is shifted more upstream at Re´=10 million (second wing image from top). In addition, the flow pattern shows more turbulent wedges due to a higher sensitivity of the boundary layer with respect to 3D roughness. The same fact can be observed when further increasing Re´ to 12 million (third wing image from top in Fig.19). For a Reynolds number of 17 million at least (bottom image in Fig.19) the transition line has moved very close to the leading edge in the midspan and tip region, superimposed by a row of small turbulent wedges. Near the wings root, laminar-turbulent boundary layer transition already occurs at the leading edge.

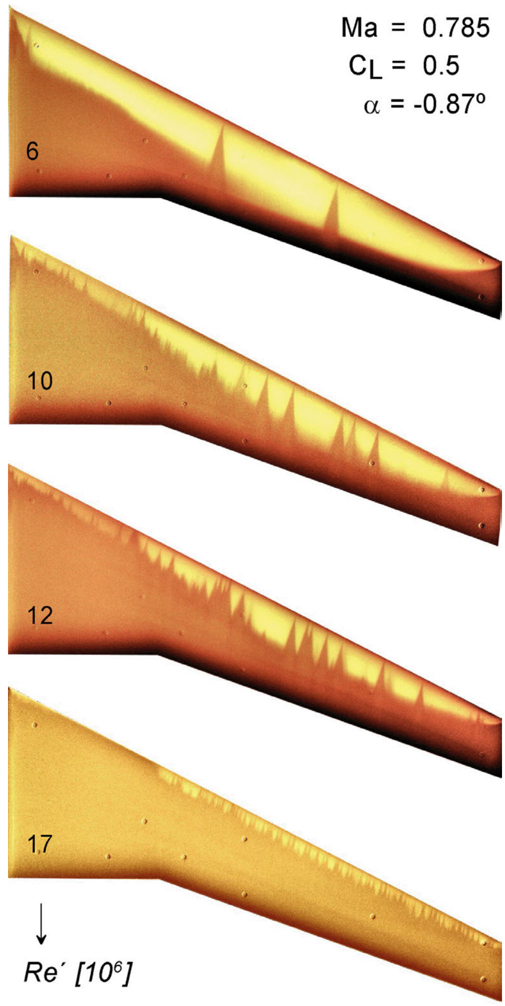

Figure 19: Development of transition line with increasing Re´. Reynolds numbers are realized using different temperatures T´ and tunnel pressures p_t (see Table1 for details).

Transition Pattern for Different Lift Coefficients

The appearance of the transition pattern with respect to a change in C_L is shown in Figure 20. Note, that a 'change in C_L' here means varying angle of attack α, which is also given in the figures. Images for C_L= 0.0, 0.4 and 0.5 were taken at the beginning of the second test campaign, after the impact holes on the wing were repaired and the nose polished again. Therefore these result images show merely the 'natural' boundary layer transition, without being influenced by a row of turbulent wedges caused by roughness around the leading edge (LE). The image corresponding to C_L= 0.3 was taken during the first test, thus, showing three turbulent wedges caused by impact holes.

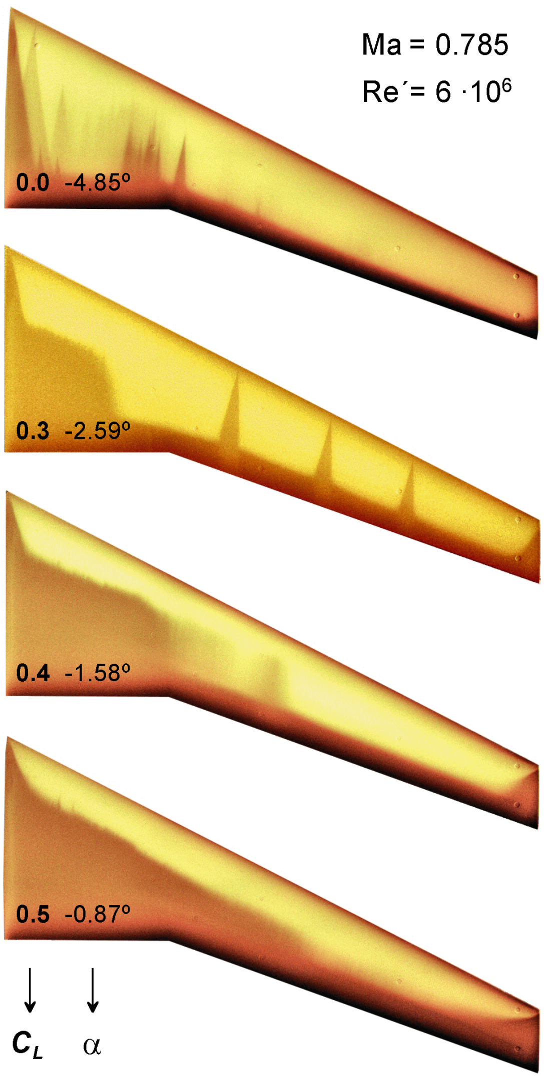

Figure 20: Development of transition line with increasing angle of attack α . Re´= 6 $\cdot 10^6$, T´=170K, pt = 121 kPa..

Comparison of TSP Covered LE and 'Paintless' LE

After repetition of some data points from the first test, the model cart was transported to the VTCR and the paint was removed from the leading edge of the wing. Figure 21 shows two images with 'paintless' leading edge with the C_L= 0.4 and 0.5. These images can be compared directly with the corresponding wing images in Figure 20 which were taken with the TSP still on the wing's leading edge.

Since the 'repaired' leading edge shows transition images without any wedge shaped structures for Re´= 6 million (see figure 20, bottom wing image), no further improvement could be expected by removing the paint from the leading edge. However, the situation has become worse for the case with removed paint. In the case of C_L= 0.5, again turbulent wedges occurred and for C_L= 0.4, the transition pattern has changed dramatically compared to Figure 20. This can be caused not only by the different roughness of the leading edge. The changeover from the metallic surface at the nose of the wing to the painted surface can change the receptivity of the boundary layer. Thus, causing the instability to be amplified more upstream. In the case of C_L= 0.4, the flow field seems to be very sensitive with respect to the 2D disturbance given by the changeover from 'paintless' to painted wing surface.

More detailed information on the boundary layer transition of the DLR F4 wing can be obtained when doing further image evaluation.

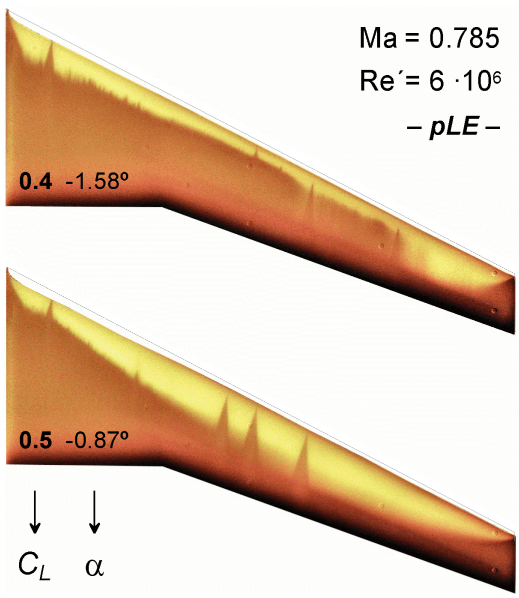

Figure 21: Transition images at C_L= 0.4 and 0.5, with the TSP paint removed from the wing's leading edge.

OUTLOOK

So far, no detailed evaluation with respect to the determination of the transition point $(x/c)_{tr}$ has been carried out. To increase accuracy, this should be undertaken together with a 3D evaluation of the images, using the numerical grid for the wing. By knowing the marker positions, it is possible to 'map' the 2D images to the 3D surface grid. Errors coming from the viewing angle of the camera and from lens distortion etc. will be corrected by DLR's ToPas-Software. A detailed (3D) evaluation of transition lines and comparison to existing experimental and numerical data will be given soon.

CONCLUSION

The application of a temperature-sensitive paint based technique for transition detection has been successfully demonstrated in the commercial ETW wind tunnel. Using TSP paint from NAL (Japan) and the modified DLR PSP/TSP measurement system, transition images of high quality have been obtained. Nevertheless, care needs to be exercised in choosing the temperature step since positive and negative steps can give different results. This means the temperature change itself may influence the instability causing the laminar-turbulent boundary layer transition. Furthermore, the actual realization of temperature changes may differ in different cryogenic wind tunnels. With this in mind, and choosing the 'right' temperature step, the TSP method has proved to be a powerful tool for transition detection in a large cryogenic wind tunnel facility. Compared to IR measurement under cryogenic conditions, the TSP technique is much easier to handle. Images acquired with TSP show higher resolution and more details in the transition pattern in comparison to IR imaging. Ongoing advancement in CCD technology provides the opportunity to improve the results by using a camera with higher resolution and increased dynamic range. The cryogenic TSP paint developed by NAL (Japan) shows a very good sensitivity in the range $110K < T < 180K$ and the capability to attain the high surface smoothness necessary for cryogenic testing. In addition, it shows the desired robustness and was able to withstand several cool-down and warm-up cycles. The DLR PSP/TSP system was successfully adapted to the specific conditions encountered at ETW. The newly developed excitation light source and the OMT-CCD camera worked successfully, even under the exceptional condition of p_t = 450 kPa. The instruments were operated reliably during two tests series and the image data transfer from camera to PC using fiber optic cabling has worked well from the beginning. Furthermore, the preliminary adjustment of all instrumentation in the mock-up at DLR was a great benefit with the resulting installation at ETW just 'plug and play'.

REFERENCES

1) R.H.Engler, K. Hartmann, I. Troyanovski, A.Vollan "Description and assessment of a new optical pressure measurement system (OPMS) demonstrated in the high speed wind tunnel of DLR in Göttingen" DLR-FB 92-24, 1-66 (1992)

2) R.H. Engler, Chr. Klein, "First Results Using the New DLR PSP System -Intensity and Lifetime Measurements", Conference 'Wind Tunnels and Wind Tunnel Test Techniques', Cambridge UK, (1997) ISBN 185768 048 0

3) R.H. Engler, Chr. Klein, "PSP-Intensity and Lifetime Measurements for Steady and Nonsteady Flow". 90th Symposium on Advanced Non-Intrusive Instrumentation for Propulsion Engines, Brussels, (1997) AGARD-CP-598, ISBN 92-836-0055-X.

4) J.A. Tizard, "ETW User Guide" ETW/D/95001 (1995)

5) Campbell, B., Liu, T. and Sullivan, J. 1994, "Temperature Sensitive Fluorescent Paint Systems", AIAA Paper 94-2483.

6) Liu, T., Campbell, B., Burns, S., and Sullivan, J. 1997, "Temperature- and Pressure-sensitive luminescent paints in aerodynamics", Applied Mechanics Reviews, Vol. 50, No. 4, 227-246.

7) Gartenberg, E. and Wright, R. E., "Boundary-Layer Transition Detection with Infrared Imaging Emphasizing Cryogenic Applications", AIAA Journal, Vol. 32, No. 9, 1994, pp. 1875-1882.

8) Gartenberg, E., Johnson, W. G., Jr. Johnson, C. B., Carraway, D. L., and Wright, R. E., "Transition Detection Studies in the Cryogenic Environment", AIAA Paper 90-3024, Aug. 1990.

9) Asai, K., Kanda, H., Kunimasu,K., Liu, T., and Sullivan, J "Boundary-Layer Transition Detection in a Cryogenic Wind Tunnel Using Luminescent Paint", J. Aircraft, Vol. 34, No. 1, 1997,34-42.

10) Iijima, Y., Egami, Y., Nishizawa, A., Asai, K., Fey, U. and Engler, R. H., 2003, "Optimization of Temperature-Sensitive Paint Formulation for Large-Scale Cryogenic Wind Tunnels". 20th International Congress on Instrumentation in Aerospace Simulation Facilities (ICIASF).